Ferroelectric block copolymers: from self-assembly towards potential application

Terzic, Ivan

CHAPTER 2

2

CuAAC Click Chemistry: A Versatile Approach Towards PVDF-based Block Copolymers

Part of this chapter was published in: *Polym. Chem.* **2018**, *9*, 3714.

Abstract

Alkyne/azide end terminated PVDF homopolymers were synthesized via free-radical polymerization using functional benzoyl peroxides as initiators. This approach allows the preparation of PVDF triblock copolymers with various functional blocks (polystyrene, poly(N-isopropylacrylamide) and poly(tert-butyl acrylate)) and tunable crystallization behavior using copper(I)-catalyzed azide-alkyne cyclo-addition.

2.1 Introduction

Electroactive polymers that change shape when triggered by an external electric field have attracted much interest over the past decades as highly promising candidates for various electronic devices.[1–3] In particular, poly(vinylidene fluoride) (PVDF)-based ferroelectric polymers are widely studied because of their large polarization, high dielectric constant and low dielectric losses.[4–6] Moreover, these polymers possess high thermal stability and desirable chemical inertness. The synthesis of block copolymers containing PVDF attracts a growing research attention as a promising strategy to introduce new functionalities into the polymer and to improve existing or to gain completely new properties.[7–9] Furthermore, their ability to self-assemble into well-ordered structures in solution and in solid state can be used for the preparation of various nanostructured materials or advanced nanocomposites.[7,10–12]

Although PVDF based block copolymers present highly valuable materials, their synthesis still remains a difficult task to achieve. The two main strategies to produce these materials are the synthesis of PVDF telomers followed by chain extension via ATRP[13,14] and reversible deactivation radical polymerization (RDRP) techniques, such as iodine transfer polymerization (ITP)[9,15] and reversible addition-fragmentation chain transfer (RAFT) polymerization using xanthate agents[16–18]. The first method results in low molecular weight block copolymers with bimodal distribution. Additionally, ATRP leads to the formation of undesirable graft copolymers by the addition of propagating chains to PVDF double bonds caused by dehydrofluorination.[19] However, head-to-head coupling of VDF during RDRP prevents the preparation of high molecular weight polymers due to accumulation of less reactive -CF_2-CH_2-X (X=I or xanthate) chain ends during the reaction.[20,21] The build-up of inactive polymer chains for block copolymer formation is overcome by adding $Mn(CO)_5$• radicals that can reactivate all iodine terminated chain ends.[22,23] In addition, Ameduri's group proved that -CF_2-CH_2-XA chain ends can start the polymerization of vinyl acetate, albeit at a slower rate.[16] Again, both methods have faced new problems, mostly concerning the molecular weight of the PVDF that is low for the successful film formation and practical application. Moreover, in the second case, the RAFT polymerization is limited to only less activated monomers.

For these reasons, it would be of great interest to have alternative methods for synthesizing PVDF-based block copolymers. In 2007, Wang's group reported the synthesis of PVDF and its copolymers with various well-defined end groups and relatively high end group fidelity (1.8-1.9) by using benzoyl peroxide(BPO)-based functional initiators.[24] Our group further improved this strategy for the preparation of PVDF-based block copolymers. Owing to its robustness, modularity and high yields under relatively mild conditions, a copper(I)-catalyzed azide-alkyne cyclo-addition (CuAAC) was employed to prepare PLLA-*b*-PVDF-*b*-

PLLA double-crystalline block copolymers.[25] The similar approach is used by Vukicevic *et al*. and Guerre *et al*., where azide terminated PVDF, either made via ITP or RAFT, is applied for the preparation of block copolymers.[7,26] The main idea of this widely used methodology is to obtain block copolymers by covalently bonding pre-synthesized 'clickable' building blocks.[27] Even though exemplified by few specific block copolymers, CuAAC of telechelic PVDF and any other desirable block represents a promising strategy to synthesize PVDF-based block copolymers for advanced applications.

2.2 Experimental section

2.2.1 Materials

Styrene (Acros Organics, 99%) and *tert*-butyl acrylate (*t*BA, Acros Organics, 99%) were dried overnight over CaH_2 and distilled under reduced pressure. *N*-isopropylacrylamide (NIPAAm, TCI, >98%) was recrystallized twice from hexane prior to use. 2,2'-Azobis(2-methylpropionitrile) (AIBN, Fluka, 98+%) was recrystallized twice from methanol. Copper(I) bromide (Sigma-Aldrich, 98%) was stirred for 1h in glacial acetic acid and then filtered and washed with ethanol and diethyl ether before drying under vacuum. The RAFT agents 2-(dodecylthiocarbonothioylthio)-2-methylpropionic acid (DDMAT), 2-(dodecylthiocarbonothioylthio)-2-methylpropionic acid 3-azido-1-propanol ester (CTA-azide) and 2-(dodecylthiocarbonothioylthio)-2-methylpropionic acid propargyl ester (CTA-alkyne) were prepared according to literature procedures.[28,29] Vinylidene fluoride (VDF, Synquest Labs, 98%), Oxalyl chloride (Acros, 98%), 4-(chloromethyl)benzoic acid (TCI, 98%), 4-((trimethylsilyl)ethynyl)benzoic acid (Sigma-Aldrich), lithium peroxide (Li_2O_2, Acros, 95%), 1,1,4,7,7-pentamethyldiethylenetriamine (PMDETA, Acros, 99+%), 1-dodecanethiol (TCI, >95.0%), tricaprylylmethylammonium chloride (Aliquat 336, TCI), carbon disulfide (Acros Organics, 99.9%), sodium hydroxide (Acros Organics, 98%), hydrochloric acid (Boom, 37%), propargyl alcohol (Acros Organics, 99%), 3-bromo-1-propanol (Acros, 97%), *N*-(3-Dimethylaminopropyl)-*N'*-ethylcarbodiimide hydrochloride (EDCI·HCl, TCI, >98%), 4-(dimethylamino)pyridine (Sigma-Aldrich, >99%), sodium azide (Sigma-Aldrich, >99.5%), , *N*,*N*-dimethylformamide (DMF, Acros Organics, anhydrous, 99.8%), dichloromethane (DCM, Acros Organics, ≥99.8%) were used as received. All other solvents were analytical grade.

2.2.2 Synthesis of 4-(chloromethyl)benzoyl peroxide

To a stirred solution of 4-(chloromethyl)benzoic acid (5 g, 29.5 mmol) in 25 mL of anhydrous DCM, oxalyl chloride (2.7 mL, 31.5 mmol) and few drops of anhydrous DMF were added at 0 °C. The reaction mixture was left to stir for 2 h at room temperature, after which the solvent was removed *in vacuo*. The remaining residue was dissolved in a mixture of n-hexane:Et_2O (50 mL 1:1) and slowly added to a vigorously stirred water solution of Li_2O_2 (1.75 g, 37.5

mmol in 25 mL) at 0 °C. After 3 h, the reaction mixture was diluted with chloroform and washed twice with water. Subsequently, the aqueous phase was extracted two times with chloroform. The combined organic phases were dried over $MgSO_4$ and the solvent was removed *in vacuo*. Recrystallization from chloroform yielded white needle-shaped crystals. ^{1}H-NMR (400 MHz, $CDCl_3$): δ= 8.07 (d, 4H, –Ar*H*), 7.56 (d, 4H, –Ar*H*), 4.64 (s, 4H, –PhCH_2Cl).

2.2.3 Synthesis of 4-((trimethylsilyl)ethynyl)benzoyl peroxide

To a slurry of 4-((trimethylsilyl) ethynyl) benzoic acid (5 g, 23 mmol) in 25 mL of anhydrous DCM, oxalyl chloride (2.2 mL, 25 mmol) and few drops of anhydrous DMF were added at 0 °C. The reaction mixture was left to stir for 2.5 h at room temperature, after which the solvent was removed *in vacuo*. The remaining residue was dissolved in a mixture of n-hexane:Et_2O (50 mL 1:1) and slowly added to a vigorously stirred water solution of Li_2O_2 (1.75 g, 37.5 mmol in 25 mL) at 0 °C. After 3 h, the reaction mixture was diluted with chloroform and washed twice with water. After this, the aqueous phase was extracted two times with chloroform. The combined organic phases were dried over $MgSO_4$ and the solvent was removed *in vacuo*. Precipitation from chloroform (20 mL) in methanol (100 mL) yielded a white product. ^{1}H-NMR (400 MHz, $CDCl_3$): δ= 7.99 (d, 4H, –Ar*H*), 7.57 (d, 4H, –Ar*H*), 0.27 (s, 18H, –Si–(CH_3)$_3$).

2.2.4 Synthesis of chlorine-terminated PVDF

A solution of 4-(chloromethyl)benzoyl peroxide (1 g, 3.0 mmol) in 300 mL of anhydrous acetonitrile was introduced into a 600 mL Parr (model 4568) high pressure reactor and purged with N_2 for 30 min. 20 bar of VDF was subsequently transferred in the reactor at room temperature. The temperature inside reactor was increased to 90 °C and the reaction mixture was stirred at 500 rpm for additional 3 hours. The reactor was cooled down by water to room temperature and depressurized to remove unreacted monomer. The solvent was removed *in vacuo* and the obtained solid was washed multiple times with chloroform to remove the initiator residues. The polymer was finally dried *in vacuo* at 45 °C to obtain a white product. ^{1}H-NMR (400 MHz, acetone-d_6): δ = 8.07 (d, –Ar*H*), 7.65 (d, –Ar*H*), 4.80 (s, –PhCH_2Cl), 4.68 (m, –COOCH_2CF_2–),3.10-2.70 (m, –CF_2CH_2–CF_2CH_2–, head-to-tail), 2.40-2.20 (m, –CF_2CH_2–CH_2CF_2–, tail-to-tail). ^{19}F-NMR (400 MHz, acetone-d_6): δ = 92.4(–CH_2CF_2–CH_2CF_2–CH_2CF_2–, head-to-tail), 96.2 (–CH_2CF_2–CF_2CH_2–CH_2CF_2–CH_2CF_2–), 114.7 (–CH_2CF_2–CH_2CF_2–CF_2CH_2–), 117.0 (–CH_2CF_2–CF_2CH_2–CH_2CF_2–).

2.2.5 Synthesis of azide-terminated PVDF

Chlorine-terminated PVDF (5 g, 0.34 mmol) and NaN_3 (448 mg, 6.89 mmol) were dissolved in 60 mL of DMF and stirred overnight at 60 °C. The polymer solution was concentrated and precipitated three times in MeOH:water (1:1). Subsequent drying of the light-yellow polymer *in vacuo* at 45 °C yielded azide terminated PVDF. ^{1}H-NMR (400 MHz, acetone-d_6): δ = 8.07 (d, –Ar*H*), 7.65 (d, –Ar*H*), 4.68 (m, –COOCH_2CF_2–), 4.60 (s, –PhCH_2N$_3$), 3.10-2.70 (m, –CF_2CH_2–CF_2CH_2–, head-to-tail), 2.40-2.20 (m, –CF_2CH_2–CH_2CF_2–, tail-to-tail).

2.2.6 Synthesis of (TMS-alkyne)-terminated PVDF

A solution of 4-((trimethylsilyl)ethynyl)benzoyl peroxide (1.3 g, 3.0 mmol) in 300 mL of anhydrous acetonitrile was introduced into a 600 mL Parr (model 4568) high pressure reactor and purged with N_2 for 30 min. 20 bar of VDF was subsequently transferred in the reactor at room temperature. The temperature inside reactor was increased to 90 °C and the reaction mixture was stirred at 500 rpm for additional 3 hours. The reactor was cooled down by water to room temperature and depressurized to remove unreacted monomer. The solvent was removed *in vacuo* and the obtained solid was washed multiple times with chloroform to remove the initiator residues. The polymer was finally dried *in vacuo* at room temperature to obtain a light-yellow product. ^{1}H-NMR (400 MHz, acetone-d_6): δ = 7.99 (d, Ar*H*), 7.63 (d, Ar*H*), 4.68 (m, -COO-CH_2CF$_2$-), 3.10-2.70 (m, –CF$_2$CH_2–CF$_2$CH_2–, head-to-tail), 2.40-2.20 (m, –CF$_2$CH_2–CH_2CF$_2$–, tail-to-tail), 0.22 (s, –Si–(CH_3)$_3$). ^{19}F-NMR (400 MHz, acetone-d_6): δ = 92.4(–CH$_2$CF$_2$–CH$_2$CF_2–CH$_2$CF$_2$–, head-to-tail), 96.2 (–CH$_2$CF$_2$–CF$_2$CH$_2$–CH$_2$CF_2–CH$_2$CF$_2$–), 114.7 (–CH$_2$CF$_2$–CH$_2$CF_2–CF$_2$CH$_2$–), 117.0 (–CH$_2$CF$_2$–CF_2CH$_2$–CH$_2$CF$_2$–).

2.2.7 Synthesis of alkyne-terminated PVDF

DBU (49.8 µL, 0.33 mmol) was added to a solution of (TMS-alkyne)-terminated PVDF (2 g, 0.16 mmol) in 200 mL of a mixture of acetonitrile:water (19:1 vol:vol). The reaction mixture was stirred for 2 hours at 60 °C. The solvent was removed *in vacuo* and the polymer was precipitated from DMF in a mixture of MeOH:water (1:1). After filtration the polymer was thoroughly washed with MeOH and DCM and finally dried *in vacuo* at room temperature to yield a light-brown polymer. ^{1}H-NMR (400 MHz, acetone-d_6): δ = 8.01 (d, Ar*H*), 7.66 (d, Ar*H*), 4.68 (m, -COO-CH_2CF$_2$-), 4.51 (s, -C*H*, alkyne), 3.10-2.70 (m, –CF$_2$CH_2–CF$_2$CH_2–, head-to-tail), 2.40-2.20 (m, –CF$_2$CH_2–CH_2CF$_2$–, tail-to-tail).

2.2.8 Synthesis of alkyne/azide-terminated PS

A typical procedure of the RAFT polymerization of styrene is as follows. Styrene monomer (9.6 mL, 84 mmol), RAFT agent (CTA-alkyne or CTA-azide) and AIBN in a molar ratio 700:1:0.1 were added to a dried Schlenk tube. The mixture was subjected to at least three freeze-pump-thaw cycles and placed in an oil bath preheated to 70 °C. After reacting for 6 h, the reaction was terminated by cooling in liquid N_2 and the solution was precipitated in a large excess of methanol. The polymer was collected via filtration and reprecipitated two more times from chloroform by methanol. The resulting polymer was dried overnight *in vacuo* at room temperature to remove all traces of residual solvent.

Alkyne-PS

^{1}H-NMR (400 MHz, CDCl$_3$): δ = 7.40-6.25 (m, C$_6$H$_5$), 4.83 (m, -S(C=S)S-C*H*(Ar)-), 4.09 (m, -COO-CH_2-), 3.27 (-CH_2-S(C=S)S-), 2.71 (s, -C*H*, alkyne) , 2.40-1.20 (m, -CH_2C*H*(Ar)-), 0.99-0.81 (m, -alkyl).

Azide-PS

^{1}H-NMR (400 MHz, $CDCl_3$): δ = 7.40-6.25 (m, C_6H_5), 4.83 (m, -S(C=S)S-C*H*(Ar)-), 4.15 (m, -COO-CH_2-), 3.27 (-CH_2-S(C=S)S-), 2.40-1.20 (m, -CH_2C*H*(Ar)-), 0.99-0.81 (m, -alkyl).

2.2.9 Synthesis of alkyne/azide-terminated PtBA

In a 25 ml Schlenk tube, monomer *t*BA (2 mL, 13.6 mmol), RAFT agent (CTA-alkyne or CTA-azide) and AIBN (at molar ratio 100:1:0.15) were dissolved in 4 mL of anhydrous DMF. After three freeze-pump-thaw cycles, the polymer mixture was placed in an oil bath at 70 °C and stirred for the next 2 h. The reaction was terminated by rapid cooling using liquid N_2 and the polymer was isolated by precipitation three times from DMF into a 20-fold excess of cold MeOH:water (1:1). The obtained yellow powder was dried *in vacuo* at room temperature for 2 days.

Alkyne-P*t*BA

^{1}H-NMR (400 MHz, $CDCl_3$): δ = 4.64 (m, –COO-CH_2–), 3.27 (t, –CH_2-S(C=S)S–), 2.87 (s, –C*H*, alkyne) 2.20 (m, –CH_2CH-(COO*t*Bu)), 1.80 (m, –CH$_2$C*H*-(COO*t*Bu)), 1.40 (m, – (COO*tBu*)), 0.85 (m, -alkyl).

Azide- P*t*BA

^{1}H-NMR (400 MHz, $CDCl_3$): δ = 4.20 (m, –COO-CH_2–), 3.40 (t, –CH_2-S(C=S)S–), 2.20 (m, –CH_2CH-(COO*t*Bu)), 1.80 (m, –CH$_2$C*H*-(COO*t*Bu)), 1.40 (m, – (COO*tBu*)), 0.85 (m, -alkyl).

2.2.10 Synthesis of alkyne/azide-terminated PNIPAAm

Anhydrous DMF (4 mL), NIPAAm (1.54 g, 13.6 mmol), RAFT agent (CTA-alkyne or CTA-azide) and AIBN (at molar ratio 100:1:0.15) were introduced into a pre-dried Schlenk tube and subjected to three freeze-pump-thaw cycles. After backfilling the Schlenk tube with nitrogen, the reaction proceeded at 70 °C for 2 h. The reaction mixture was cooled down using liquid N_2 and precipitated three times into diethyl ether. The obtained product was dried for a few hours *in vacuo* at room temperature.

Alkyne-PNIPAAm

^{1}H-NMR (400 MHz, $CDCl_3$): δ = 6.10 (s, -N*H*-CH(CH$_3$)$_2$), 4.65 (m, –COO-CH_2–), 4.00 (m, -NH-C*H*(CH$_3$)$_2$) 3.32 (t, –CH_2-S(C=S)S–), 2.10 (m, –CH$_2$C*H*-COO-), 1.60 (m, –CH_2CH-COO-), 1.13 (m, -NH-CH(CH_3)$_2$), 0.86 (t, -alkyl).

Azide-PNIPAAm

^{1}H-NMR (400 MHz, $CDCl_3$): δ = 6.10 (s, -N*H*-CH(CH$_3$)$_2$), 4.20 (m, –COO-CH_2–), 4.00 (m, -NH-C*H*(CH$_3$)$_2$) 3.32 (t, –CH_2-S(C=S)S–), 2.10 (m, –CH$_2$C*H*-COO-), 1.60 (m, –CH_2CH-COO-), 1.13 (m, -NH-CH(CH_3)$_2$), 0.86 (t, -alkyl).

2.2.11 General procedure for the preparation of PVDF based block copolymers

A general route for the Cu-catalyzed alkyne azide cycloaddition (CuAAC) used for the preparation of block copolymers is described below. The azide/alkyne-terminated PVDF (300 mg, 0.021mmol for azide-terminated, 0.024 mmol for alkyne-terminated PVDF), the other polymer (PS, P*t*BA or PNIPAAm) and CuBr were added into dried Schlenk tube in a molar ratio [PVDF]:[polymer]:[CuBr] = 1:2.6:4. After performing a degassing procedure (three repetitive cycles of evacuating and backfilling with N_2), 4 mL of anhydrous DMF was added, followed by PMDETA (30 µL, 0.14 mmol). The reaction was allowed to stir for 3 days at 60 °C and afterwards terminated by exposition to air. The reaction mixture was filtered through a short neutral alumina column in order to remove copper catalyst. The solution was concentrated under reduced pressure and precipitated in a 20-fold excess of nonsolvent (MeOH:water (1:1) for the block copolymers containing PS and P*t*BA, and cold diethyl ether for the block copolymer with PNIPAAm). After filtration the product was collected via filtration and dried overnight *in vacuo* at room temperature.

2.2.12 Purification of the PVDF based block copolymers

Having in mind that we used excess of the other polymer compared to PVDF end groups, in order to have a complete reaction and to avoid PS, P*t*BA or PNIPAAm homopolymer contaminations, the residual excess of these polymers had to be removed to get pure block copolymers. The unreacted homopolymers were removed by selective dissolution in a relatively good solvent for them, but nonsolvent for block copolymers (Table 2.1). Previously dried products were mixed with the selective solvent and subjected to centrifugation (5 min at 4500 rpm). Unreacted homopolymer remained dissolved while the block copolymer separated on the bottom. The procedure was repeated a few times until all homopolymer was removed. The products collected after centrifugation were furthermore dried *in vacuo* at 45 °C in order to get pure block copolymers.

Table 2.1 Selective solvents used for purification of block copolymers.

Block copolymer	Selective solvent
PS-*b*-PVDF-*b*-PS	Diethyl ether
P*t*BA-*b*-PVDF-*b*-P*t*BA	Diethyl ether or methanol
PNIPAAm-*b*-PVDF-*b*-PNIPAAm	Water

2.2.13 Characterization

Nuclear Magnetic Resonance Spectroscopy *(^{1}H-NMR)* was performed on a 400 MHz Varian (VXR) spectrometer at a room temperature.

Gel Permeation Chromatography (GPC) of PVDF and its block copolymers was performed in DMF (containing 0.01 M LiBr) using a Viscotek GPCmax equipped with a model 302 TDA

detectors and two columns (Agilent Technologies-PolarGel-L and M, 8 μm 30 cm) at a flow rate of 1.0 mL min^{-1} and 50 °C. Prior to the measurements, the block copolymer samples were passed through alumina column to remove copper catalyst that can induce the aggregation of the block copolymer samples on the column, and filtrated through PTFE filter with 0,20 μm pore size. Narrow dispersity PMMA standards (Polymer Laboratories) were used for constructing the universal calibration curve applied for determining molecular weights. The molecular weight and the dispersity of PS, P*t*BA and PNIPAAm were determined using triple detection method (refractive index, viscosity and light scattering) using THF, stabilized with BHT, as the eluent at a flow rate 1.0 mL min^{-1} at 35 °C. The separation was carried out by utilizing two PLgel 5 μm MIXED-C, 300 mm columns (Agilent Technologies) calibrated with narrow disperse polystyrene standards (Agilent Technologies and Polymer Laboratories). Predetermined refractive indices (d*n*/d*c*) of 0.185, 0.0512 and 0.034 mL g^{-1} were used for PS, P*t*BA and PNIPAAm, respectively.

Differential Scanning Calorimetry (DSC) thermograms were recorded on a TA Instruments DSC Q1000 by heating the sample to 200 °C, then equilibrating for 30 min before cooling to room temperature at 10 °C min^{-1} and then heating again to 200 °C at 10 °C min^{-1}.

Small-angle X-ray scattering (SAXS) measurements were carried out at the Dutch-Belgium Beamline (DUBBLE) station BM26B of the European Synchrotron Radiation Facility (ESRF) in Grenoble, France. [30,31] The sample to detector distance was ca. 3.5 m. The scattering vector q is defined as $q = 4\pi/\lambda(\sin\theta)$ with 2θ being the scattering angle and λ the wavelength of the X-rays (1.03 Å).

Transmission electron microscopy (TEM) was performed on a Philips CM12 transmission electron microscope operating at an accelerating voltage of 120 kV. Prior to imaging, polymer films were obtained *via* casting of block polymer solutions in DMF into a glass Petri dish. The solvent was allowed to evaporate at 45 °C for two days. Obtained films were thermally annealed at 200 °C for 30 min and subsequently cooled down to room temperature at 10 °C min^{-1}. A piece of the block copolymer film was embedded in epoxy resin (Epofix, Electron Microscopy Sciences) and subsequently microtomed using a Leica Ultracut UCT-ultramicrotome in order to prepare ultrathin sections (ca. 80 nm). No additional staining of the samples was performed.

2.3 Results and Discussion

The current Chapter reports the application and versatility of CuAAC in the preparation of PVDF-based block copolymers. The crucial step of this methodology is the synthesis of

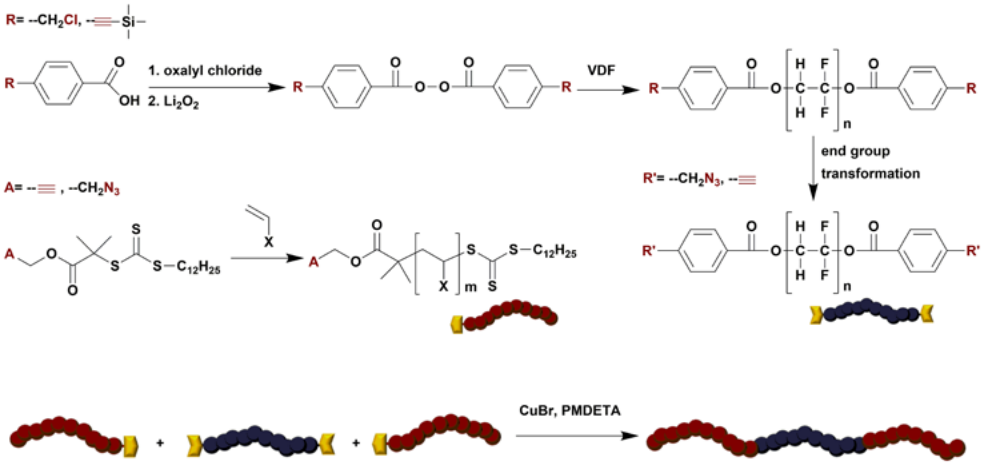

Scheme 2.1 Schematic representation of the synthesis of PVDF-based block copolymers using CuAAc click-coupling.

telechelic azide and alkyne PVDF polymers which are used for further coupling. To achieve this task, we decided to use free radical polymerization initiated by functional BPOs, bearing in mind that the termination reaction in radical polymerization of fluorinated monomers occurs exclusively through the combination of radicals.[32]

Using the approach outlined in Scheme 2.1, the functional group of the benzoyl peroxide is present at both ends of the PVDF chains and can be used for subsequent reactions. In order to obtain azide terminated polymers, a chlorine functionalized initiator was used and after polymerization converted to azide, whereas an initiator having trimethylsilyl (TMS) protected ethynyl groups allowed successful preparation of alkyne terminated PVDF. Both BPO initiators were prepared from commercially available reagents via acylation of Li_2O_2 with functional benzoyl chloride, and further recrystallization. Polymers were obtained by solution polymerization of VDF in acetonitrile at 90 °C. Using acetonitrile as solvent is beneficial to minimize chain transfer to solvent, while the choice of the temperature was considered optimal taking in account molecular weight and yield. As exemplified in Figure 2.1, the ^{1}H-NMR spectrum of chlorine terminated PVDF reveals signals centered at 2.95 and 2.35 ppm, characteristic for head-to-tail and tail-to-tail sequences in the polymer backbone.[32] The signals of phenyl protons at 8.07 and 7.65 ppm and methylene protons next to halogen atom at 4.80 ppm together with the appearance of the triplet centered at 4.68 ppm that corresponds to final methylene group bonded to the ester group from the initiator clearly show the incorporation of initiator fragments at the chain ends. Additionally, the small peaks at 6.29 and 1.79 ppm associated with $-CH_2-CF_2H$ and $-CF_2-CH_3$ short branches that resulted from intramolecular branching reactions (backbiting) can also be

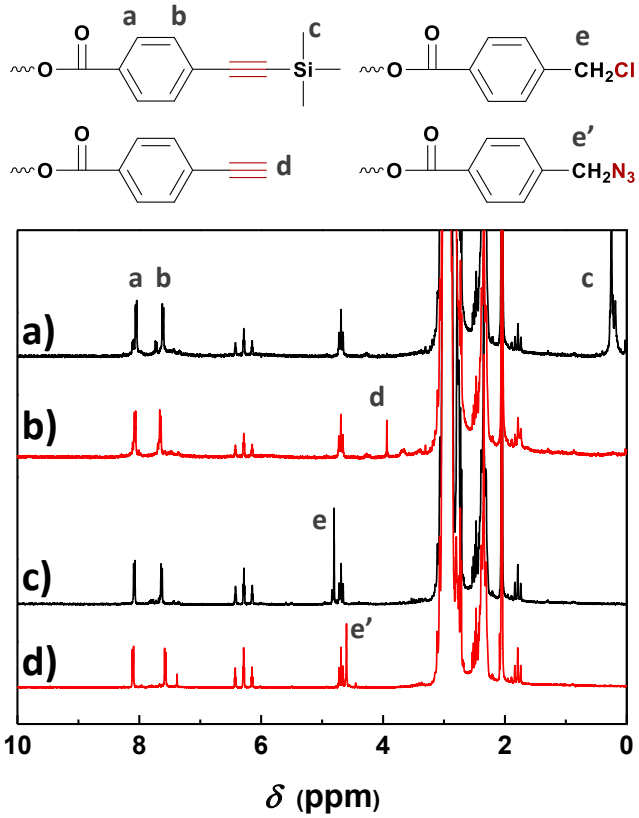

Figure 2.1 ^{1}H-NMR spectra in acetone-d_6 of (a) (TMS-alkyne) terminated PVDF, (b) alkyne terminated PVDF, (c) chlorine terminated PVDF and (d) azide terminated PVDF showing successful preparation of telechelic PVDFs.

observed.[11,24,25,33] After stirring chlorine terminated PVDF with excess of sodium azide in DMF overnight and further purification, light yellow azide terminated PVDF is obtained. The complete shift of the signal corresponding to methylene protons linked to the halogen atom from 4.80 to 4.60 ppm demonstrates the quantitative exchange of the end groups.

Following the same polymerization procedure as for the synthesis of chlorine terminated PVDF, polymers with terminal alkyne groups are prepared. The initiator used for the synthesis is functionalized with TMS protected ethynyl groups in order to avoid side reactions. The ^{1}H-NMR spectrum of (TMS-alkyne)-PVDF (Figure 2.1a,b), with no methylene protons, but with the existence of TMS-protecting group signal at 0.25 ppm, displays similar signals as in the case of chlorine terminated PVDF. The protecting group is cleaved by stirring the polymer with a slight excess of DBU in acetonitrile: water mixture for 2h at 60 °C. The ^{1}H-NMR spectrum of alkyne terminated PVDF provides clear evidence for the complete deprotection

Table 2.2 Molecular weight characteristics of the prepared polymers.

	N_3-PVDF-N_3 method		≡-PVDF-≡ method	
Product	$M_{n,GPC}$ (kg mol^{-1})	*Đ*	$M_{n,GPC}$ (kg mol^{-1})	*Đ*
PVDF	14.4	1.48	11.6	1.60
PS	8.2	1.20	9.8	1.18
P*t*BA	12.2	1.22	12.0	1.15
PNIPAAm	11.7	1.27	11.3	1.22
PS-*b*-PVDF-*b*-PS	29.5[a)]	1.60	32.2[a)]	1.98
P*t*BA-*b*-PVDF-*b*-P*t*BA	34.7[a)]	1.37	29[a)]	1.62
PNIPAAm-*b*-PVDF-*b*-PNIPAAm	36.0[a)]	1.54	31.4[a)]	1.75

[a)] Molecular weight calculated from $M_{n,GPC}$ values of PVDF taking in the account ratio between the blocks calculated using ^{1}H-NMR. The determination of molecular weight of block copolymers using GPC is not accurate bearing in mind that PVDF gives negative, while other polymers positive RI signal.

due to the disappearance of the TMS signal and the appearance of a new signal that belongs to the ethynyl proton at 4.51 ppm. During cleavage, the polymer color changes from light-yellow to light-brown. This suggests that a dehydrofluorination reaction takes place parallel to the removal of protecting groups. However, it has been observed before that with as little as 0.1 % of dehydrofluorination, PVDF turns into a deep black polymer, as a result of the formation of conjugated C=C bonds within the polymer backbone.[34] Moreover, the absence of a C=C bond signal at 6 ppm in the ^{1}H-NMR spectrum is additional evidence that this unwanted phenomenon is present in a negligible amount. Both polymers, synthesized using different initiators, have similar dispersity of around 1.5, while the molecular weight of the polymer synthesized using a chlorine containing initiator is higher. The main reason for small dispersity values lies in the absence of the disproportionation reaction together with an exhausting washing procedure that removes small molecular weight fractions. Additionally, we believe that the higher concentration of the alkyne containing initiator, caused by either better solubility and/or higher half-life compared to the initiator with the chlorine groups, is responsible for the difference in the molecular weight between polymers.

To evaluate the universality of this concept for block copolymer synthesis, three different polymers bearing complementary end groups, whether alkyne or azide, were synthesized. Polystyrene is chosen as a common polymer to test the alkyne/azide click reaction. On the other hand, poly(*tert*-butyl acrylate) (P*t*BA) is regularly used as a precursor for preparation of poly(acrylic acid), while poly(*N*-isopropylacrylamide) (PNIPAAm) is especially interesting due to its thermally responsive behavior in water. Both polymers, poly(acrylic acid) and PNIPAAm, are soluble in an aqueous environment and the preparation of block copolymers with PVDF represents a promising approach for the formation of pH and temperature responsive materials via self-assembly in solution.

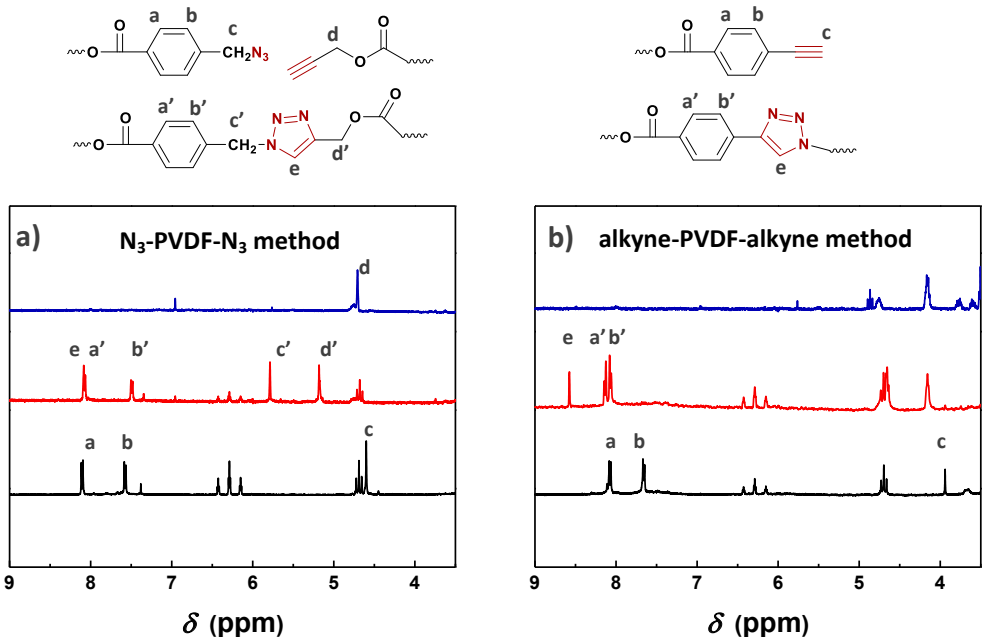

Figure 2.2 ^{1}H-NMR spectra in acetone-d_6 showing the successful preparation of P*t*BA-*b*-PVDF-*b*-P*t*BA block copolymers starting from (a) azide terminated PVDF and (b) alkyne terminated PVDF.

All of the above-mentioned polymers are synthesized using RAFT, as it serves as a convenient and versatile technique with the possibility to obtain narrow molecular weight polymers with well-defined structures and end groups.[35] The reactions are performed in the presence of RAFT agents, 2-(dodecylthiocarbonothioylthio)-2-methylpropionic acid propargyl (CTA-alkyne) or 3-azido-1-propanol ester (CTA-azide) at 70 °C. The use of the RAFT agents results in the formation of alkyne- or azide- terminated polymers that can be used in the CuAAC reaction with PVDF homopolymers. The molecular weight characteristics of the synthesized polymers are depicted in Table 2.2.

The last step to achieve PVDF-based triblock copolymers is coupling of already prepared end functionalized polymers using copper(I)-catalyzed azide-alkyne cyclo-addition reaction. All reactions are performed in DMF at 60 °C in the presence of a copper(I) bromide-pentamethyldiethylenetriamine (PMDETA) complex. In order to gain full conversion of PVDF end groups and to avoid contamination of block copolymers with an unreacted PVDF homopolymer, a 1.3-fold excess of the other polymer is used. After 3 days, the reaction is stopped and the catalyst is removed by passing the polymer solution through a neutral aluminum oxide plug. Since one of the polymers had been used in excess, we washed the dried crude product with a selective solvent-good solvent for homopolymer (PS, P*t*BA and PNIPAAm) but a bad solvent for PVDF and the block copolymer. After a few centrifugation

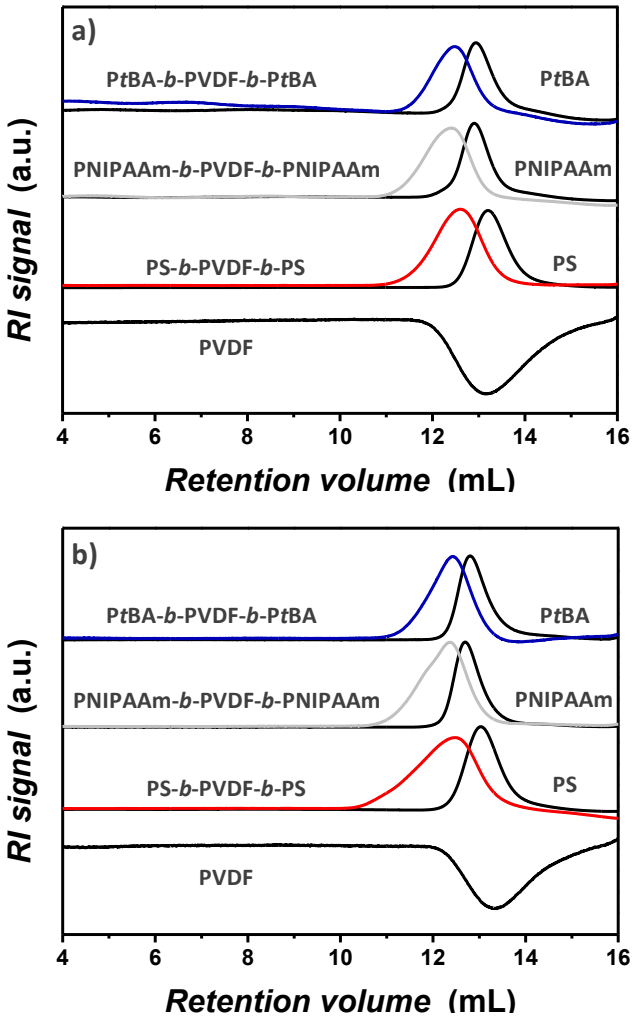

Figure 2.3 GPC traces of homopolymers and block copolymers indicating preparation of the pure block copolymers starting from (a) azide terminated PVDF and (b) alkyne terminated PVDF.

steps and solvent exchanges, the crude product is isolated and dried to give a pure block copolymer. The formation of the block copolymer and its purity is examined using ^{1}H-NMR spectroscopy and gel permeation chromatography (GPC). The changes in the ^{1}H-NMR spectra will only be explained for the reaction with P*t*BA, since the other block copolymers show similar results. After the reaction, if the azide terminated PVDF is used, the signals of the methylene protons next to the azide group of PVDF and next to the alkyne group of P*t*BA are both completely shifted from 4.60 and 4.71 ppm to 5.79 and 5.17 ppm, respectively, whereas a new signal for the triazole proton appears at 8.09 ppm (Figure 2.2a). This all confirms the full conversion of PVDF into the triblock copolymer. Similar observations in

the coupling reaction are made when alkyne terminated PVDF is used. A strong downfield shift of the signal assigned to the aromatic protons next to the alkyne group from 7.65 to 8.06 ppm, together with a total disappearance of the singlet corresponding to the terminal alkyne proton indicates a complete reaction (Figure 2.2b).

Besides ^{1}H-NMR spectroscopy, the successfulness of the click reaction is additionally proven by comparing GPC signals of homo- and block copolymers (Figure 2.3). Independently of the end group combination and polymer type used in the reaction, the RI signal of block copolymer shows a shift to lower retention volumes compared to the homopolymer. Additionally, no signals related to unreacted homopolymers were observed demonstrating the preparation of pure block copolymers. Bearing in mind a small deviation from an ideal functionality of 2, an increase of the dispersity values of block copolymers compared to homopolymers is expected. The impossibility to achieve the ideal functionality is caused by the presence of transfer reactions during polymerization. The transfer reactions, in this case, may occur to the solvent, to the initiator and to the polymer. As abovementioned, the formation of $-CH_2-CF_2H$ and $-CF_2-CH_3$ end groups is observed using ^{1}H-NMR (Figure 2.1). They origin from the chain transfer reactions, mostly to the polymer (backbiting and transfer to another polymer chain). Signals of end groups that would appear after chain transfer to initiator or solvent are not detected by ^{1}H-NMR. Despite the presence of unwanted reactions during conventional free radical polymerization, the functionality still stays close to the ideal case (1.8-1.9). [24,25] Taking this into account, a mixture of triblock and diblock copolymers is obtained under these conditions, which gives rise to higher dispersity. The effect of polydispersity on the block copolymer self-assembly is still not fully explored, although recent studies showed a positive effect of polydispersity on the microphase separation.[36,37] In the work of Mahanthappa and co-workers, the increased polydispersity of the middle block in ABA block copolymer drove the formation of even richer phase behavior compared to the narrow-dispersed analogues.[38] This suggests that block copolymers synthesized using the method reported in this communication, even though having a higher polydispersity, can be used as a platform to obtain piezoelectric nanostructures *via* microphase separation.

The ferroelectric properties of PVDF are a direct consequence of its crystalline structure, indicating the importance of block copolymer crystallization studies. Block copolymers can show high diversity of crystallization behavior, depending on their molecular characteristics. [39] The crystallization nature of block copolymers upon cooling down from the melt, as well as the impact of the amorphous polymer structure on PVDF crystallization was studied using DSC. The polymers were heated to 200 °C, kept for 30 minutes and subsequently cooled down to room temperature. Figure 2.4a,b depict the DSC cooling and heating curves of PVDF and its block copolymers indicating that crystallization temperature and degree of crystallinity are strongly influenced by the nature of the amorphous block. Conversely, no

significant effect of the molecular characteristics on the melting temperature is observed. Such a variety of pathways in the crystallization is a direct consequence of two parameters: the interaction between blocks and the glass transition temperature of the amorphous block. In the case of PNIPAAm-*b*-PVDF-*b*-PNIPAAm, complete miscibility between PVDF and PNIPAAm above the melting point of PVDF is observed by using small angle X-ray scattering (SAXS) (Figure 2.4c).[30,31] The high miscibility of these two polymers is expected due to the hydrogen bond formation between the carbonyl group of PNIPAAm and the -CH_2 groups of PVDF. PNIPAAm has a high T_g (T_g=116 °C) that strongly affects the crystallization behavior of the block copolymer. The vitrification of the amorphous component occurs at a similar temperature as the crystallization of PVDF homopolymer, leading to a complete disruption of crystallization. As a consequence, strong undercooling and a substantial reduction of the crystallinity are observed.

Table 2.3 Crystallization of PVDF and its block copolymers (prepared using alkyne-PVDF-alkyne).

Polymer	T_c [a] (°C)	X_c [b] (%)
PVDF	132	47
PS-*b*-PVDF-*b*-PS	53.0	21
P*t*BA-*b*-PVDF-*b*-P*t*BA	110	46
PNIPAAm-*b*-PVDF-*b*-PNIPAAm	66	4

[a] Determined from DSC thermograms. [b] Calculated using the following equation: $X_C=(\Delta H_C/f\Delta H_{100})\times100\%$. ΔH_C was determined from DSC thermograms while *f* presents weight fraction of PVDF. ΔH_{100}=104.5 J g^{-1}.

Contrary to PNIPAAm-*b*-PVDF-*b*-PNIPAAm, due to unfavorable interactions between P*t*BA or PS and PVDF, the melt of these two polymers consists of PVDF spheres embedded inside a PS or P*t*BA matrix (Figure 2.4b,c). The large contrast in their crystallization behavior lies in their different glass transition temperatures. The T_g value for P*t*BA (T_g=43 °C) is not high enough to prevent break-out crystallization of PVDF, and the formation of the lamellar structure consisting of PVDF crystals and amorphous part made of PVDF and P*t*BA is inevitable (Figure 2.4d). The degree of the crystallinity is equal to that of pure PVDF, while the reduction of crystallization temperature from 132 °C to 110 °C is attributed to the hindering effect of P*t*BA (Table 2.3). On the contrary, after the solidification of the PS matrix, the crystallization of PVDF develops inside 3D confined spherical nanodomains (Figure 2.4c). As a consequence, the crystallization temperature is reduced to only 53 °C, while the degree of crystallinity dropped two times compared to the homopolymer, still highly exceeding the values for PNIPAAm-*b*-PVDF-*b*-PNIPAAm. This example demonstrates the intriguing effect of microphase separation on crystallization which allows it to occur at lower temperatures, while preserving satisfactory crystallinity of the sample. It is evident that the abovementioned crystallization behavior is limited to the reported compositions only and that different ratios between the blocks together with the morphology formed in

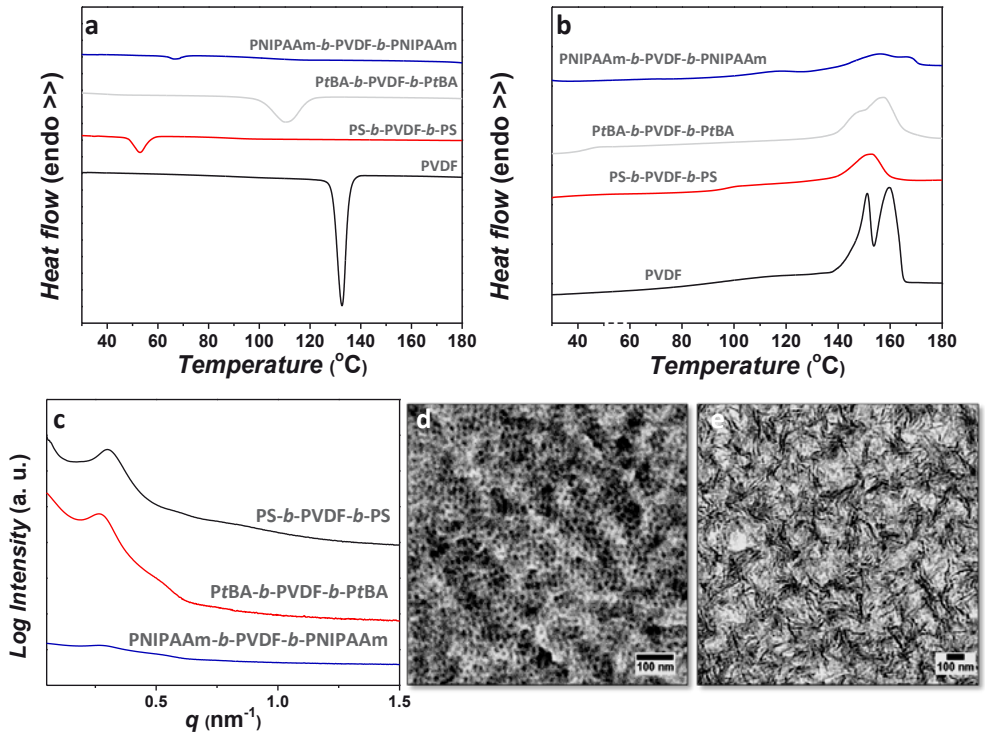

Figure 2.4 (a) DSC cooling, (b) heating curves of PVDF and block copolymers obtained during cooling (heating) with 10 °C min^{-1}, (c) SAXS patterns of block copolymers recorded at 200 °C, (d) TEM image of PS-*b*-PVDF-*b*-PS after cooling from the melt indicates confined crystallization, (e) TEM image of P*t*BA-*b*-PVDF-*b*-P*t*BA after break-out crystallization.

the melt can lead to completely different crystallization events.[40] Nevertheless, this study is out of the scope of this Chapter and will be examined in the Chapter 4.

2.4 Conclusion

In summary, telechelic PVDF polymers, bearing alkyne or azide end groups are synthesized using functional benzoyl peroxide initiators. These polymers are used for the preparation of different triblock copolymers with PS, P*t*BA and PNIPAAm using a copper(I)-catalyzed azide-alkyne cyclo-addition. Both approaches yield pure block copolymer, free of unreacted homopolymers. This synthetic route presents an alternative method to RAFT and ITP for the formation of well-defined block copolymers. The obtained block copolymers show a rich crystallization behavior, highlighting the strong effect of the amorphous block's molecular structure on crystal formation. They demonstrate either phase segregation or

homogeneous melt, which significantly impacts their crystallization behavior. PNIPAAm-*b*-PVDF-*b*-PNIPAAm block copolymer forms a homogeneous melt and it is characterized by complete disruption of the crystallization. Conversely, the outcome of crystallization for the phase separated block copolymers is dependent on the glass transition temperature (T_g) of the non-crystalline block. A high T_g of polystyrene copolymer induced a confined crystallization inside spherical domains, while the break-out crystallization takes place for the block copolymer containing low T_g P*t*BA.

2.5 References

[1] X. Chen, X. Han, Q.-D. Shen, *Adv. Electron. Mater.* **2017**, *3*, 1600460.
[2] M. Josowicz, J. Janata, in *Applications of Electroactive Polymers*, Springer, Dordrecht, **1993**, pp. 310–343.
[3] L. Zhu, Q. Wang, *Macromolecules* **2012**, *45*, 2937.
[4] E. Fukada, T. Furukawa, *Ultrasonics* **1981**, *19*, 31.
[5] Y. Lu, J. Claude, B. Neese, Q. Zhang, Q. Wang, *J. Am. Chem. Soc.* **2006**, *128*, 8120.
[6] B. Ameduri, *Chem. Rev.* **2009**, *109*, 6632.
[7] M. Guerre, M. Semsarilar, C. Totée, G. Silly, B. Améduri, V. Ladmiral, *Polym. Chem.* **2017**, *8*, 5203.
[8] F. Guan, J. Wang, L. Yang, J.-K. Tseng, K. Han, Q. Wang, L. Zhu, *Macromolecules* **2011**, *44*, 2190.
[9] A. Meskini, M. Raihane, I. Stevenson-Royaud, G. Boiteux, G. Seytre, B. Ameduri, *J. Non-Cryst. Solids* **2010**, *356*, 688.
[10] Y. Wu, L. Chen, X. Sun, J. Xu, G. Gu, J. Qian, *J. Saudi Chem. Soc.***2017**, *21*, 713.
[11] V. S. D. Voet, M. Tichelaar, S. Tanase, M. C. Mittelmeijer-Hazeleger, G. ten Brinke, K. Loos, *Nanoscale* **2013**, *5*, 184.
[12] V. S. D. Voet, D. Hermida-Merino, G. ten Brinke, K. Loos, *RSC Adv.* **2013**, *3*, 7938.
[13] M. Destarac, K. Matyjaszewski, E. Silverman, B. Ameduri, B. Boutevin, *Macromolecules* **2000**, *33*, 4613.
[14] E. M. W. Tsang, Z. Shi, S. Holdcroft, *Macromolecules* **2011**, *44*, 8845.
[15] D. Valade, C. Boyer, B. Ameduri, B. Boutevin, *Macromolecules* **2006**, *39*, 8639.
[16] M. Guerre, S. M. W. Rahaman, B. Améduri, R. Poli, V. Ladmiral, *Polym. Chem.* **2016**, *7*, 6918.
[17] Y. Patil, B. Ameduri, *Polym. Chem.* **2013**, *4*, 2783.
[18] M. Guerre, M. Uchiyama, E. Folgado, M. Semsarilar, B. Améduri, K. Satoh, M. Kamigaito, V. Ladmiral, *ACS Macro Lett.* **2017**, *6*, 393.
[19] M. Henze, D. Mädge, O. Prucker, J. Rühe, *Macromolecules* **2014**, *47*, 2929.
[20] M. Guerre, S. M. W. Rahaman, B. Améduri, R. Poli, V. Ladmiral, *Macromolecules* **2016**, *49*, 5386.
[21] C. Boyer, D. Valade, P. Lacroix-Desmazes, B. Ameduri, B. Boutevin, *J. Polym. Sci., Part A: Polym. Chem.* **2006**, *44*, 5763.
[22] A. D. Asandei, O. I. Adebolu, C. P. Simpson, *J. Am. Chem. Soc.* **2012**, *134*, 6080.
[23] A. D. Asandei, *Chem. Rev.* **2016**, *116*, 2244.
[24] K. Li, S. Liang, Y. Lu, Q. Wang, *Macromolecules* **2007**, *40*, 4121.
[25] V. S. D. Voet, G. O. R. A. van Ekenstein, N. L. Meereboer, A. H. Hofman, G. ten Brinke, K. Loos, *Polym. Chem.* **2014**, *5*, 2219.
[26] R. Vukićević, U. Schwadtke, S. Schmücker, P. Schäfer, D. Kuckling, S. Beuermann, *Polym. Chem.* **2012**, *3*, 409.
[27] D. Quémener, T. P. Davis, C. Barner-Kowollik, M. H. Stenzel, *Chem. Commun.* **2006**, *0*, 5051.
[28] J. T. Lai, D. Filla, R. Shea, *Macromolecules* **2002**, *35*, 6754.
[29] R. Ranjan, W. J. Brittain, *Macromol. Rapid Commun.* **2007**, *28*, 2084.
[30] M. Borsboom, W. Bras, I. Cerjak, D. Detollenaere, D. Glastra van Loon, P. Goedtkindt, M. Konijnenburg, P. Lassing, Y. K. Levine, B. Munneke, M. Oversluizen, R. van Tol, E. Vlieg, *J. Synchrotron Radiat.* **1998**, *5*, 518.
[31] W. Bras, I. P. Dolbnya, D. Detollenaere, R. van Tol, M. Malfois, G. N. Greaves, A. J. Ryan, E. Heeley, *J. Appl. Crystallogr* **2003**, *36*, 791.
[32] J. Guiot, B. Ameduri, B. Boutevin, *Macromolecules* **2002**, *35*, 8694.
[33] M. Pianca, E. Barchiesi, G. Esposto, S. Radice, *J. Fluorine Chem.* **1999**, *95*, 71.
[34] A. Taguet, L. Sauguet, B. Ameduri, B. Boutevin, *J. Fluorine Chem.* **2007**, *128*, 619.
[35]) Y. K. Chong, T. P. T. Le, G. Moad, E. Rizzardo, S. H. Thang, *Macromolecules* **1999**, *32*, 2071.
[36] N. A. Lynd, M. A. Hillmyer, *Macromolecules* **2005**, *38*, 8803.
[37] M. E. Vanderlaan, M. A. Hillmyer, *Macromolecules* **2016**, *49*, 8031.

[38] J. M. Widin, A. K. Schmitt, A. L. Schmitt, K. Im, M. K. Mahanthappa, *J. Am. Chem. Soc.* **2012**, *134*, 3834.
[39] Y.-L. Loo, R. A. Register, A. J. Ryan, *Macromolecules* **2002**, *35*, 2365.
[40] M.-C. Lin, H.-L. Chen, W.-F. Lin, P.-S. Huang, J.-C. Tsai, *J. Phys. Chem. B* **2012**, *116*, 12357.